Ophthalmol Ther (2024) 13:3161–3173
https://doi.org/10.1007/s40123-024-01054-2

ORIGINAL RESEARCH

Intraretinal Microvascular Abnormalities in Eyes with Advanced Stages of Nonproliferative Diabetic Retinopathy: Comparison Between UWF-FFA, CFP, and OCTA—The RICHARD Study

Ana R. Santos · Marta Lopes · Torcato Santos · Débora Reste-Ferreira · Inês P. Marques · Taffeta C. N. Yamaguchi · Telmo Miranda · Luís Mendes · António C. V. Martinho · Liz Pearce · José Cunha-Vaz

Received: June 24, 2024 / Accepted: October 4, 2024 / Published online: October 26, 2024

ABSTRACT

***Introduction*:** This study aimed to evaluate intraretinal microvascular abnormalities (IRMA) in eyes with advanced nonproliferative diabetic retinopathy (NPDR) using multimodal approach in co-located areas focusing on central retina (up to 50°) and to look at possible correlations between IRMA and other structural changes, like ischemia and presence of microaneurysms.

***Methods*:** The RICHARD study (NCT05112445) included 60 eyes from 60 patients with type 2 diabetes with moderate-severe NPDR, diabetic retinopathy severity levels 43, 47, and 53 (DRSS). IRMA were defined as capillary tortuosity covering a minimum circular area of 300 µm (calculated to correspond to the Early Treatment Diabetic Retinopathy Study standard photo 8A) and were identified using multimodal imaging with distinct fields of view (FoV): color fundus photography (CFP) using a Topcon TRC-50DX camera (Topcon Medical Systems, Japan), Optos California ultra wide field fundus fluorescein angiography (UWF-FFA) (Optos plc, UK), and swept-source optical coherence tomography angiography (SS-OCTA) (PLEX® Elite 9000, ZEISS, USA). Different areas of the retina were examined: central macula (up to 20°) and posterior pole (between 20° and 50°).

Prior Presentation: This work was presented at the ARVO 2024 Annual Meeting and EAsDEC 2024 Conference. Lopes M, Santos AR, Santos T, Reste-Ferreira D, Marques I, Yamaguchi T, Miranda T, Pearce L, Cunha-Vaz J, Identification of intraretinal microvascular abnormalities in eyes with advanced stages of NPDR: comparison between ultra wide field FA, CFP and OCTA, Investigative Ophthalmology & Visual Science June 2024, Vol. 65, 1770. 34th Meeting of the European Association for Diabetic Eye Complications (EAsDEC) University of Milan, Milan, Italy 30th May–1st June 2024. European Journal of Ophthalmology. 2024;34(1_suppl):S1–S40. https://doi.org/10.1177/11206721241244945.

Supplementary Information The online version contains supplementary material available at https://doi.org/10.1007/s40123-024-01054-2.

A. R. Santos · M. Lopes · T. Santos · D. Reste-Ferreira · I. P. Marques · T. Miranda · L. Mendes · A. C. V. Martinho · J. Cunha-Vaz (✉)
AIBILI - Association for Innovation and Biomedical Research On Light and Image, Coimbra, Portugal
e-mail: cunhavaz@aibili.pt

A. R. Santos · I. P. Marques
CORC - Coimbra Ophthalmology Reading Centre, Coimbra, Portugal

A. R. Santos
Center for Translational Health and Medical Biotechnology Research (TBIO)/Health Research Network (RISE-Health), ESS, Polytechnic of Porto, Porto, Portugal

Results: Multimodal imaging was used to identify IRMA in co-located areas (FoV < 50°) including UWF-FFA, CFP, and SS-OCTA. In eyes with DRSS levels 47 and 53, IRMA were identified in both areas of the retina, while in eyes with DRSS level 43, IRMA were detected only outside of the central macula (FoV > 20°). Our results show that when evaluating the presence of IRMA (FoV < 50°), UWF-FFA detected 203 IRMA, SS-OCTA detected 133 IRMA, and CFP detected 104 IRMA. Our results also show that the presence of IRMA was positively associated with presence of microaneurysms.
Conclusions: Identification of IRMA in eyes with advanced NPDR is better achieved by UWF-FFA than CFP and SS-OCTA. A statistically significant correlation was found between the presence of IRMA and the increase in number of microaneurysms.
Trial Registration: ClinicalTrials.gov, identifier NCT05112445.

Keywords: Diabetes; Retinopathy; Intraretinal microvascular abnormalities; Fluorescein angiography; Fundus photography; Wide field optical coherence tomography angiography; Microaneurysms

Key Summary Points

Why carry out this study?

Tortuous intraretinal vascular segments known as intraretinal microvascular abnormalities (IRMA) are a known risk factor for proliferative diabetic retinopathy development with vision-threatening complications.

The purpose of this study is to identify and compare IRMA in co-located areas focusing on central retina (up to 50°) using different imaging modalities in eyes with advanced nonproliferative diabetic retinopathy.

We also investigate possible correlations between IRMA and other structural changes, namely ischemia and presence of microaneurysms.

What was learned from the study?

Our study shows that increased number of IRMA is associated with increased severity of diabetic retinopathy.

Identification of IRMA in eyes with advanced NPDR focusing on central retina (field of view [FoV] < 50°) was better achieved by ultra wide field fundus fluorescein angiography than swept-source optical coherence tomography angiography and color fundus photography.

Another relevant finding of our study is a significant correlation between the presence of IRMA and the increase in number of microaneurysms.

INTRODUCTION

Diabetes mellitus is a major public health problem worldwide causing significant morbidity and mortality and having considerable socioeconomic implications. A 2021 report by the

I. P. Marques

Coimbra Institute for Clinical and Biomedical Research (iCBR), Faculty of Medicine, University of Coimbra, Coimbra, Portugal

T. C. N. Yamaguchi
Boehringer Ingelheim, GmBH, Ingelheim am Rhein, Germany

A. C. V. Martinho
Eye Clinic, University Hospital Basel, Basel, Switzerland

L. Pearce
Institute of Ophthalmology, University College London, London, United Kingdom

J. Cunha-Vaz
Faculty of Medicine, University of Coimbra, Coimbra, Portugal

International Diabetes Federation estimated that by 2045 there will be 783 million people worldwide with diabetes [1]. Approximately one-third of people with diabetes develop signs of diabetic retinopathy (DR), with 10% developing vision-threatening complications [2–4].

In 1991, the Early Treatment of Diabetic Retinopathy Study (ETDRS) used standardized photographs, 8A and 8B, to define intraretinal microvascular abnormalities (IRMA) as tortuous intraretinal vascular segments located in standard fields 3–7, varying in caliber from barely visible to 31 µm per ETDRS. IRMA appear in more severe stages of DR leading to a higher risk of proliferative diabetic retinopathy (PDR) development [5]. Therefore, the classification and detection of IRMA may provide significant insights as clinical markers for the progression of DR and the associated risk of vision-threatening complications. Fluorescein angiography (FA) is an invasive procedure but it is still considered the standard diagnosis of IRMA [6]. Multimodal imaging of IRMA is expected to allow their characterization and improved identification. Optos California (Optos plc, Dunfermline, UK) ultra wide field fundus fluorescein angiography (UWF-FFA) is a recent device that allows the performance of FA in UWF images. This device allows improved visualization of the peripheral retina compared to the standard 7-field ETDRS (82% vs 30%) [7–10]. OCT-angiography (OCTA) is a non-invasive method offering high-resolution angiograms for evaluation of microvascular features and has been shown to be useful in DR to detect IRMA with higher resolution compared to conventional FA and color fundus photography (CFP). It has been reported that approximately 50% more IRMA are detected with OCTA than with color fundus imaging [11, 12].

The aim of this study is to evaluate IRMA in eyes with advanced nonproliferative diabetic retinopathy (NPDR), diabetic retinopathy severity levels 43, 47, and 53 (ETDRS-DRSS), to identify and compare IRMA in co-located areas focusing on central retina, up to 50°, using different imaging modalities, namely UWF-FFA (invasive method) and CFP and OCTA (non-invasive methods). We also look at possible correlations between IRMA and other structural changes, namely ischemia and presence of microaneurysms.

METHODS

Study Population

The RICHARD study (clinicaltrials.gov identifier NCT05112445), a non-interventional prospective cohort study, was approved by the Association for Innovation and Biomedical Research on Light and Image (AIBILI) Ethics Committee (CE 240 RICHARD) in accordance with the tenets of Declaration of Helsinki. The participants provided their written informed consent to participate in this study.

The participants were considered according to specific inclusion and exclusion criteria. Eligible patients met the following inclusion criteria: (1) type 2 diabetes according to World Health Organization, (2) patients over 18 years of age, (3) DRSS levels between 43 and 53 based on the ETDRS criteria complemented with UWF-fundus photography (UWF-FP) imaging, (4) refraction with an absolute spherical equivalent less than 5 diopters (positive or negative) to minimize possible imaging distortions affecting the quality of the images, and (5) able to provide informed consent. Exclusion criteria were as follows: any retinal vascular disease that may interfere with study results (including clinically significant macular edema), glaucoma, age-related macular degeneration, vitreomacular disease, any eye surgery within a period of 6 months before the baseline visit, previous laser treatment or intravitreal injections, dilation of pupil < 5 mm and uncontrolled glycated hemoglobin A1C level > 12% (107.66 mmol/mol). Only one eye per patient was included. The eye with more severe DRSS grading was chosen. However, when both eyes had the same DRSS level, the eye with the higher ischemic index on UWF-FFA was chosen.

Subjects

This analysis included 60 patients, one eye per patient, diagnosed with type 2 diabetes with moderate to severe NPDR (DRSS levels 43, 47, and 53).

Demographic and clinical information for all participants including age, sex, diabetes duration, vital signs (height, weight, body mass index, systolic and diastolic blood pressure, and heart rate) and laboratory characteristics (glycated hemoglobin, cholesterol, and triglycerides) were recorded. All participants underwent comprehensive ophthalmological examination, including best corrected visual acuity (BCVA) evaluation, slit-lamp bio-microscopy, indirect ophthalmoscopy, intraocular pressure (IOP) measurement, and fundus imaging.

Identification of IRMA

IRMA were defined in 1991 by ETDRS Research Group as tortuous intraretinal vascular segments, varying in caliber from barely visible to 31 µm per ETDRS [5]. According to the ETDRS severity scale, IRMA are present in more severe stages of NPDR (ETDRS levels ≥ 43B). In this analysis, IRMA were identified as capillary tortuosities covering a minimum equivalent circular area of 300 µm calculated to correspond to ETDRS standard photo 8A.

Multimodal imaging was performed to identify IRMA in co-located areas focusing on central retina (up to 50°), including UWF-FFA (invasive method) and CFP (field 2) and SS-OCTA (non-invasive methods). Different zones of the retina were examined: central macula (up to 20° of the retina) and posterior pole (from 20° to 50°). We also evaluated the presence of IRMA in areas beyond 50° of the retina in UWF-FFA (from 50° to 130°). The identification of IRMA in different modalities was performed by a single grader.

Diabetic Retinopathy Severity Scale

Diabetic retinopathy severity scale grading was performed on the basis of the grading of standard seven-field CFP images obtained with 35° field of view using the Topcon TRC 50DX mydriatic retinal camera (Topcon Medical Systems, Tokyo, Japan), with a resolution of 3596 × 2448 pixels. Adequate dilation of the pupil of at least 5 mm was ensured using mydriasis (0.5% tropicamide and 0.5% phenylephrine hydrochloride topical drops) to obtain good quality images. In addition, we complemented the classification with the UWF-FP images captured using Optos California (Optos plc, Dunfermline, UK). This device's software automatically places a grid to outline the seven ETDRS fields [13, 14]. Retinal photographs for DRSS classification were evaluated by two trained graders at the Coimbra Ophthalmology Reading Centre (CORC). In the case of a discrepancy between the two retinal specialists, a senior grader provided adjudication. The Gwet's AC1 coefficient was 0.809 for DRSS classification between graders, indicating very good agreement, with a 95% confidence interval ranging from 0.719 to 0.899. The DRSS was classified as moderate NPDR—DRSS level 43, moderately severe NPDR—DRSS level 47, and severe NPDR – DRSS level 53.

Ultra Wide Field Fundus Fluorescein Angiography

Ultra wide field fundus fluorescein angiography images were captured using the Optos California device (Optos plc, Dunfermline, UK). This system is a confocal scanning laser ophthalmoscope with an ellipsoidal mirror able to capture 130° of the retinal fundus in a single image without requiring bright illumination lighting or a contact lens, and in some patients, pupillary dilation. This device uses a blue argon laser at 488 nm to excite sodium fluorescein and captures a 4000 × 4000 pixel image through a 500-nm barrier filter. This single scan takes 0.25 s to provide approximately 20-pixel resolution per degree [15, 16]. FA requires the intravenous injection of fluorescein dye. Patients were injected with 1.5 ml of 100 mg/ml (20%) sodium fluorescein and early phase images were analyzed to calculate the percentage of total ischemic index and to identify IRMA. Ischemic index percentage is obtained by the total area of retinal ischemia divided by total area of visible retina [17].

Swept-Source Optical Coherence Tomography Angiography

All participants were imaged with PLEX® Elite 9000 (ZEISS, Dublin, CA, USA) SS-OCTA device using the Angio 15 mm × 15 mm acquisition protocol. This SS-OCTA operates a tunable 1060-nm laser to provide an axial resolution of 6.3 µm. This acquisition protocol is able to scan 50° of the retina and provides angiography slabs images based on two repetitions of 834 B-scans with 834 A-scans with an acquisition rate of 100,000 A-scans/s [18–20].

Acquired data from this device was processed using the Macular Density v0.7.3.3 analysis protocol available on the Advanced Retina Imaging Network Hub (https://arinetworkhub.com). Acquisition data was processed to compute slab images and numerical data for the foveal avascular zone (FAZ), skeletonized vessel density (SVD) and perfusion density (PD) metrics at the superficial and deep capillary plexi (SCP and DCP). PD metrics and images are the result of the binarization of the enface angiography images and represent changes in vessel perfusion. A skeletonization of the binary images generates the SVD metrics and images to represent the number of individual capillaries that are carrying red blood cells. Its decrease indicates capillary closure [21, 22].

SVD and PD were measured in the macular area and posterior pole. Macular area, namely, central subfield (CSF, 0.5 mm radius circle centered at the fovea), inner ring (InR, 0.5–1.5 mm radius ring centered at the fovea), and outer ring (OutR, 1.5–3.0 mm radius ring centered at the fovea). In addition, the posterior pole area, namely, extended ring 1 (Ext1, 3–4.5 mm radius ring centered at the fovea), extended ring 2 (Ext2, 4.5–6 mm radius ring centered at the fovea), and extended ring 3 (Ext3, 6–7.5 mm radius ring centered at the fovea).

Microaneurysm Detection

Microaneurysm (MA) identification was automatically performed on CFP images (field F2—50° of the retina) using the RetmarkerDR software (Retmarker SA, Meteda Group, Rome, Italy), computer-aided diagnostic software that performs MA earmarking and identification of macular red dot-like vascular lesions [23, 24]. RetmarkerDR has been used since 2011 and RetmarkerDR Biomarker is currently certified as a class IIA medical device in Europe. RetmarkerDR software is highly conservative in order to reduce variability.

Statistical Analysis

Statistical analyses of the data were performed using STATA software, version 16.1 (StataCorp LLC, College Station, Texas, USA). *P* values less than 0.05 were considered statistically significant different.

Distribution of data normality was assessed using the Kolmogorov–Smirnov test. Percentages were reported for categorical variables and numerical variables are expressed as the mean and standard deviation.

Spearman's rank correlation was performed to assess correlation between grading parameters. The Spearman correlation coefficient (rho, ρ) was defined on the basis of strength of correlation, as very weak ($0.00 \le \rho < 0.20$), weak ($0.20 \le \rho < 0.40$), moderate ($0.40 \le \rho < 0.60$), strong ($0.60 \le \rho < 0.80$), or very strong ($0.80 \le \rho < 1.00$).

RESULTS

Baseline Characteristics

The RICHARD study included 60 eyes from 60 patients with diabetes type 2 with advanced NPDR (DRSS levels 43, 47, and 53). The mean age of patients was 67.8 ± 8.6 years (range 50–85 years) with 78% being male. At baseline, 12 eyes (20%) were classified as DRSS level 43—moderate NPDR, 36 eyes (60%) classified as DRSS level 47—moderately severe NPDR, and 12 eyes (20%) classified as DRSS level 53—severe NPDR. Demographic, clinical and ophthalmological characteristics are described in Table 1.

Table 1 Demographic, clinical, and ophthalmological characteristics of included patients

Variables	Mean ± SD or *N* (%)
Demographic and clinical characteristics	
Number of patients	60
Number of eyes	60
Sex *N* (%)	
Male	47 (78%)
Female	13 (22%)
Age (years)	67.8 ± 8.6
Duration of DR (years)	21.7 ± 7.1
Body mass index (kg/m^2)	29.5 ± 4.5
Diastolic blood pressure (mmHg)	73.5 ± 7.1
Systolic blood pressure (mmHg)	139.3 ± 11.7
Heart rate (bpm)	72.4 ± 10.8
HbA1c (%)	7.5 ± 1.1
Triglycerides (mg/dL)	141.6 ± 64.3
Total cholesterol (mg/dL)	164.6 ± 47.9
LDL cholesterol (mg/dL)	87.9 ± 38.2
HDL cholesterol (mg/dL)	48.5 ± 14.0
Ophthalmological characteristics	
Moderate NPDR—DRSS level 43	12 (20%)
Moderately severe NPDR—DRSS level 47	36 (60%)
Severe NPDR—DRSS level 53	12 (20%)
Best corrected visual acuity (letters)	83.2 ± 5.2
Intraocular pressure (mmHg)	16.9 ± 3.5
Ischemic index (%)	3.6 ± 4.1
Number of microaneurysms (N)	7.2 ± 8.00

SD standard deviation, *N* number of patients, *HbA1c* glycated hemoglobin, *LDL* low-density lipoprotein, *HDL* high-density lipoprotein, *NPDR* nonproliferative diabetic retinopathy, *DRSS* Diabetic Retinopathy Severity Scale

Identification of IRMA Using Different Imaging Modalities

Eye fundus imaging including UWF-FFA, CFP (field 2) and SS-OCTA was used to identify IRMA in 60 eyes in co-located areas, up to 50° of the retina. These results are present in Table 2. In DRSS levels 47 and 53, IRMA were identified in both areas of the retina using the three imaging modalities. In contrast, in DRSS level 43, IRMA were detected only in areas outside the central macula (field of view [FoV] > 20°). Our results show that, when analyzing the presence of IRMA

Table 2 Identification of IRMA using different imaging modalities

	Central macula up to 20°			Posterior pole from 20° to 50°			Central macula and posterior pole up to 50°		
	Eyes	T_{IRMA}	Ratio T_{IRMA} / eyes	Eyes	T_{IRMA}	Ratio T_{IRMA} / eyes	Eyes	T_{IRMA}	Ratio T_{IRMA} / eyes
CFP									
DRSS 43, *N* = 12	0 (0.0%)	0	0.0	6 (50.0%)	7	1.2	6 (50.0%)	7	1.2
DRSS 47, *N* = 36	9 (25.0%)	14	1.6	23 (63.9%)	48	2.1	24 (66.7%)	62	2.6
DRSS 53, *N* = 12	4 (33.3%)	6	1.5	8 (66.7%)	29	3.6	8 (66.7%)	35	4.4
Total, *N* = 60	13 (21.7%)	20	1.5	31 (51.7%)	84	2.7	38 (63.3%)	104	2.7
SS-OCTA									
DRSS 43, *N* = 12	0 (0.0%)	0	0.0	5 (41.7%)	11	2.2	5 (41.7%)	11	2.2
DRSS 47, *N* = 36	3 (8.3%)	3	1.0	30 (83.3%)	91	3.0	30 (83.3%)	94	3.1
DRSS 53, *N* = 12	3 (25.0%)	4	1.3	11 (91.7%)	24	2.2	11 (91.7%)	28	2.5
Total, *N* = 60	6 (10.0%)	7	1.2	46 (76.7%)	126	2.7	46 (76.7%)	133	2.9
UWF-FFA									
DRSS 43, *N* = 12	0 (0.0%)	0	0.0	6 (50.0%)	16	2.7	6 (50.0%)	16	2.7
DRSS 47, *N* = 36	6 (16.7%)	12	2.0	30 (83.3%)	100	3.3	31 (86.1%)	112	3.6
DRSS 53, *N* = 12	5 (41.7%)	11	2.2	11 (91.7%)	64	5.8	11 (91.7%)	75	6.8
Total, *N* = 60	11 (18.3%)	23	2.1	47(78.3%)	180	3.8	48 (80.0%)	203	4.2

DRSS Diabetic Retinopathy Severity Scale, *N* number, *IRMA* intraretinal microvascular abnormalities, *CFP* color fundus photography, *SS-OCTA* swept-source optical coherence tomography angiography, *UWF FFA* ultra wide field fundus fluorescein angiography, *T* total

in central retina (Fov < 50°), UWF-FFA detected 203 IRMA, while SS-OCTA detected 133 IRMA, and CFP detected 104 IRMA. In the central macula (FoV < 20°), UWF-FFA detected 23 IRMA in 11 eyes (ratio = 2.1), SS-OCTA detected 7 IRMA in 6 eyes (ratio = 1.2), and CFP detected 20 IRMA in 13 eyes (ratio = 1.5). In the posterior pole (20° < FoV < 50°), UWF-FFA detected 180 IRMA in 47 eyes (ratio = 3.8), SS-OCTA detected 126 IRMA in 46 eyes (ratio = 2.7), and CFP detected only 84 IRMA in 31 eyes (ratio = 2.7). We also evaluated the presence of IRMA in areas beyond 50° of the retina in UWF-FFA (50° < FoV < 130°). We identified 215 IRMA in 52 eyes (ratio = 4.1). Using SS-OCTA, we identified IRMA only in the superficial capillary plexus.

Localization of IRMA by Retina Quadrants

Our results show that the presence of IRMA was predominantly located outside of central macula (FoV > 20°). Topographically, IRMA were more frequently identified in superior and temporal retinal quadrants than in the others (FoV < 20°). In central retina (Fov < 50°), IRMA were more frequently identified in superior and inferior retinal quadrants than nasal and temporal quadrants. These results are shown in Supplementary Table S1.

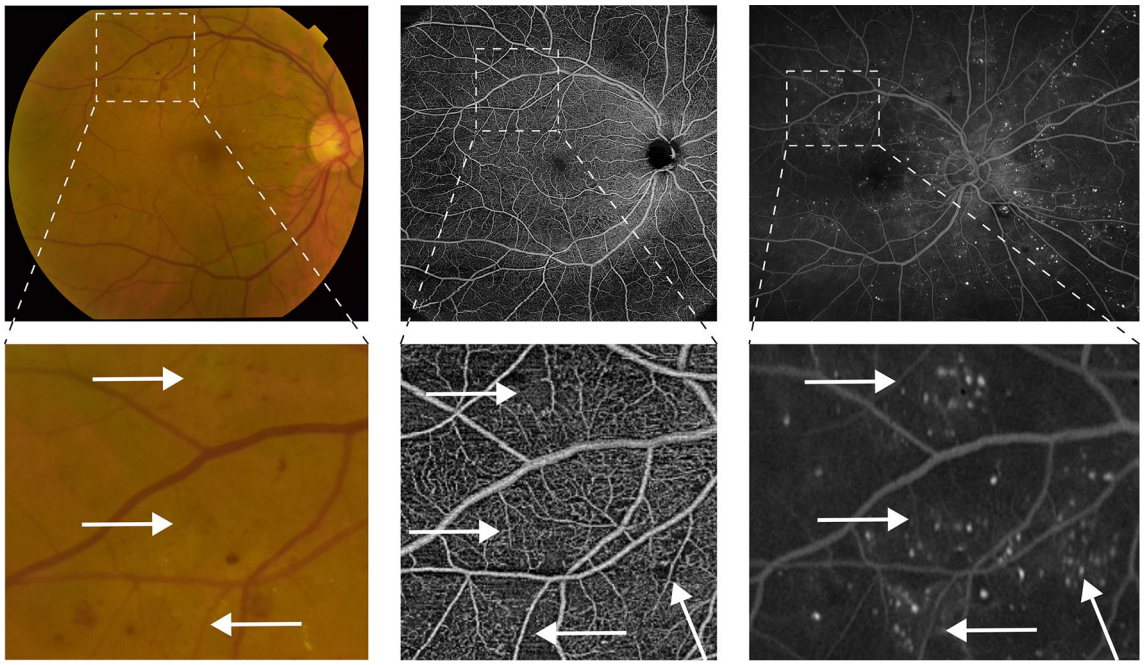

Fig. 1 Identification of IRMA in the different modalities (CFP, SS-OCTA, and UWF-FFA) with IRMA annotations at the same location. UWF-FA is cropped at the region of interest and images are shown with different magnifications to compensate for different field of view. *IRMA* intraretinal microvascular abnormalities, *CFP* color fundus photography, *UWF FFA* ultra wide field fundus fluorescein angiography, *SS-OCTA* swept-source optical coherence tomography angiography

Co-localization of IRMA: UWF-FFA Versus OCTA (FoV < 50°)

The co-localization of IRMA between UWF-FFA and SS-OCTA is illustrated in Fig. 1. When considering co-located areas, up 50° of the retina, UWF-FFA detected 203 IRMA, while SS-OCTA detected 133 IRMA. A total of 68 IRMA were identified at the same location in both imaging modalities (UWF-FFA and SS-OCTA). This correspond to 33% ($n = 68/203$) for UWF-FFA and 51% ($n = 68/133$) for SS-OCTA.

Association Between IRMA and Ischemic Index

Our results show that there is a statistically significant positive correlation between ischemic index values and the presence of IRMA in all retina quadrants. The ischemic index obtained from UWF-FFA was weakly correlated with the number of IRMA detected by CFP, UWF-FFA, or SS-OCTA. When considering only eyes with DRSS levels 47 and 53, this correlation becomes stronger (Table 3).

Association Between IRMA and OCTA

There is also a statistically significant positive correlation between capillary nonperfusion (i.e., decreasing SVD and PD) and the presence of IRMA when examining SS-OCTA images, up to 50° of the retina. Our results reach statistical significance in the temporal quadrant (IRMA with SVD for DCP: $\rho = -0.335$, $p = 0.014$ and IRMA with PD for DCP: $\rho = -0.336$, $p = 0.014$).

Table 3 Association between IRMA and ischemic index for the posterior pole (up to 50° of the retina)

IRMA identified by multimodal imaging	Ischemic index identified by UWF-FFA							
	Nasal		Inferior		Temporal		Superior	
	ρ	*p* value	*ρ*	*p* value	*ρ*	*p* value	*ρ*	*p* value
All								
IRMA identified by CFP	0.280	0.032*	0.290	0.026*	0.281	0.031*	0.352	0.006*
IRMA identified by UWF-FFA	0.260	0.047*	0.531	< 0.001*	0.386	0.003*	0.334	0.010*
IRMA identified by SS-OCTA	0.093	0.486	0.312	0.017*	0.304	0.020*	0.372	0.004*
Only ETDRS-DRSS levels 47–53								
IRMA identified by CFP	0.239	0.102	0.320	0.027*	0.322	0.026*	0.349	0.015*
IRMA identified by UWF-FFA	0.179	0.222	0.576	< 0.001*	0.437	0.002*	0.329	0.022*
IRMA identified by SS-OCTA	− 0.018	0.903	0.294	0.045*	0.335	0.021*	0.381	0.008*

Spearman correlation coefficient (ρ) was as very weak ($0.00 \le \rho < 0.20$), weak ($0.20 \le \rho < 0.40$), moderate ($0.40 \le \rho < 0.60$), strong ($0.60 \le \rho < 0.80$), or very strong ($0.80 \le \rho < 1.00$)

IRMA intraretinal microvascular abnormalities, *CFP* color fundus photography, *UWF FFA* ultra wide field fundus fluorescein angiography, *SS-OCTA* swept-source optical coherence tomography angiography, *DRSS* Diabetic Retinopathy Severity Scale

*Values represent statistically significant alterations with $p < 0.05$ using Spearman correlation

Association Between Ischemic Index and SS-OCTA

Our results showed that retinal capillary nonperfusion was identified in UWF-FFA and SS-OCTA metrics. SVD and PD metrics were weakly correlated with ischemic index in total area of the retina (ExtR2 for DCP, SVD: ρ = − 0.274, $p = 0.049$ and PD: ρ = − 0.273, $p = 0.050$). When considering only eyes with DRSS levels 47 and 53, the correlation became stronger (ExtR2 for DCP, SVD: ρ = − 0.403, $p = 0.008$ and PD: ρ = − 0.401, $p = 0.009$).

Association Between IRMA and Microaneurysms

Our results also show that the presence of IRMA was associated with presence of microaneurysms (up to 50° of the retina). Number of IRMA identified by CFP and UWF-FFA was weakly correlated with number of microaneurysms identified by CFP images counting with RetmarkerDR software (central macula, CFP: ρ = 0.256, $p = 0.048$ and UWF-FFA: ρ = 0.325, $p = 0.011$). When considering the presence of IRMA identified by SS-OCTA, the correlation became stronger (central macula, ρ = 0.496, $p < 0.001$) (Table 4).

DISCUSSION

In this study, we examined the presence of IRMA using multimodal imaging in advanced stages of preproliferative diabetic retinopathy (DRSS levels 43, 47, and 53). IRMA are defined as capillary tortuosities covering a minimum circular area of 300 µm (calculated to correspond to ETDRS standard photo 8A), based on ETDRS fundus photography [5].

Previous studies have indicated that IRMA may be more readily detected with OCTA compared to CFP [11, 12]. Our results showed, indeed, a greater number of IRMA in SS-OCTA than CFP. In addition, it has been reported that the inter-agreement between OCTA and UWF-FP to detect IRMA is moderate, and to improve the

Table 4 Association between presence of IRMA and number of MA

IRMA identified by multimodal imaging	MA identified with RetmarkerDR	
	ρ	*p* value
Central macula up to 20°		
IRMA identified by CFP	0.256	0.048*
IRMA identified by UWF FFA	0.325	0.011*
IRMA identified by SS-OCTA	0.496	< 0.001*
Posterior pole from 20° to 50°		
IRMA identified by CFP	0.069	0.599
IRMA identified by UWF FFA	− 0.009	0.948*
IRMA identified by SS-OCTA	0.272	0.036

Spearman correlation coefficient (ρ) was as very weak ($0.00 \le \rho < 0.20$), weak ($0.20 \le \rho < 0.40$), moderate ($0.40 \le \rho < 0.60$), strong ($0.60 \le \rho < 0.80$), or very strong ($0.80 \le \rho < 1.00$)

IRMA intraretinal microvascular abnormalities, *CFP* color fundus photography, *UWF FFA* ultra wide field fundus fluorescein angiography, *SS-OCTA* swept-source optical coherence tomography angiography

*Values represent statistically significant alterations with $p < 0.05$ using Spearman correlation

concordance values it is important to combine multimodal imaging devices [25]. Our study confirmed these findings.

Our study also confirms that an increased number of IRMA is associated with increased severity of diabetic retinopathy. More specifically, IRMA are present in more advanced stages of preproliferative diabetic retinopathy, DRSS levels 47 and 53, as expected by ETDRS severity classification.

Imaging of IRMA on FA and OCTA appears to correspond to the collateral shunt vessels identified originally by Cogan and Kuwabara [26] and Ashton [27], and shown to be associated with capillary closure. It is of note, however, that these studies were performed in postmortem retina specimens, without the information or identification of their degrees of retinopathy severity.

It is noteworthy that in DRSS levels 47 and 53, IRMA are identified in similar number with SS-OCTA and UWF-FFA, when considering the central retina (up to 50°). However, UWF-FFA identifies IRMA in the far periphery even in DRSS level 43. This finding needs to be examined further to see how peripheral lesions are relevant to identify eyes at hight risk of progression.

Another relevant finding of our study is that when using OCTA, IRMA were only identified in the superficial capillary plexus. This observation, previously referred by other authors [28], may help to explain the microvascular disease progression in diabetic retinopathy. The microvascular alterations appear to start in the SCP with localized areas of capillary dropout progressing later with increased involvement of the DCP and extending progressively from the center to the periphery [10, 29]. This progressive hypoperfusion of the DCP reaches maximal values and may leave only the SCP responding to the nutrition needs of the retina. It appears that to compensate for the widespread and progressive capillary closure, there is, afterwards, an angiogenic response through the formation of enlarged shunt vessels, the precursors of IRMA, which may be explained as an attempt at the re-establishment of adequate levels of oxygen availability. Indeed, the development of IRMA appears to be associated with the hyperperfusion stage of NPDR and may be the hallmark of this angiogenic response to the progressive ischemia.

A relevant observation is that although the quantification of IRMA and their degree of severity are notoriously difficult, our study shows that the presence of microaneurysms and their increase in numbers may be a reliable surrogate for the presence of IRMA [30–32]. This study also shows that there is good correspondence between ischemic index values, OCTA hypoperfusion metrics, and presence of IRMA.

One of the major limitations of this study is the small number of eyes ($N = 60$ eyes) and the unbalanced DR groups. Moreover, these patients have relatively well controlled type 2 diabetes. However, this last limitation, can be seen as an advantage as it minimizes the influence of systemic variables. We also evaluated the presence of IRMA using swept-source OCTA. The sensitivity of OCTA can vary depending on the devices,

technology, and algorithms used [33]. The identification of IRMA in peripheral areas was only performed using UWF-FFA, which is a limitation of the study.

CONCLUSIONS

IRMA appear to be good indicators of the retinal hyperperfusion response to the progressive hypoperfusion that characterizes the initial stages of diabetic retinopathy [34]. This observation suggests a clear need to identify and characterize the presence of IRMA in diabetic retina to monitor the disease progression. In addition, microaneurysm quantification appears to be a useful surrogate for the presence and degree of severity of IRMA.

Authorship. All named authors meet the International Committee of Medical Journal Editors (ICMJE) criteria for authorship for this article, take responsibility for the integrity of the work as a whole, and have given their approval for this version to be published.

Author Contributions. Ana R Santos, Marta Lopes, Torcato Santos, Débora Reste-Ferreira, Inês P Marques, Telmo Miranda, Luís Mendes and António CV Martinho designed and conducted the study, collected, analyzed and interpreted the data, wrote, revised and edited the manuscript. Taffeta CN Yamaguchi analyzed and critically reviewed the manuscript. Liz Pearce participated in the design of the study, analyzed and critically reviewed the manuscript. José Cunha-Vaz participated in the design of the study, assisted in the analysis and interpretation of the data, and wrote the manuscript. José Cunha-Vaz is the guarantor of this work and, as such, had full access to all the data in the study and takes responsibility for the integrity of the data and the accuracy of the data analysis. All authors have read and agreed to the published version of the manuscript.

Funding. RICHARD study (NCT05112445) is an Investigator Initiated Research (IIR) sponsored by AIBILI and was funded by Boehringer Ingelheim through an IIR Grant. AIBILI is responsible for initiation, conduction and management of the study, and for the writing of the manuscript. Boehringer Ingelheim provided consult, reviewed and approved this manuscript and decision to submit the manuscript for publication. No funding or sponsorship was received for the publication of this article.

Data Availability. The datasets generated during and/or analyzed during the current study are available from the corresponding author on reasonable request.

Declarations

Conflicts of Interest. Ana R Santos, Marta Lopes, Torcato Santos, Débora Reste-Ferreira, Inês P Marques, Telmo Miranda, Luís Mendes and António CV Martinho declare there are no conflicts of interest. Taffeta CN Yamaguchi is a Boehringer Ingelheim employee. Liz Pearce previously worked at Boehringer Ingelheim, participated in the design of the study. José Cunha-Vaz reports grants from Bayer, Boehringer Ingelheim and Carl Zeiss Meditec and is a consultant for Alimera Sciences, Bayer, Boehringer Ingelheim, Carl Zeiss Meditec and Roche. José Cunha-Vaz is an Editorial Board member of *Ophthalmology and Therapy*. José Cunha-Vaz was not involved in the selection of peer reviewers for the manuscript nor any of the subsequent editorial decisions.

Ethical Approval. The tenets of the Declaration of Helsinki were followed, and approval was obtained from the AIBILI Ethics Committee for Health (CE 240 RICHARD), and the trial was registered at ClinicalTrials.gov, identifier NCT05112445. Written informed consent was obtained by each participant agreeing to participate in the study.

REFERENCES

1. International Diabetes Federation. IDF diabetes atlas. 10th ed. Brussels: International Diabetes Federation; 2021.

2. Narayan KMV, Boyle JP, Geiss LS, Saaddine JB, Thompson TJ. Impact of recent increase in incidence on future diabetes burden: U.S., 2005–2050. Diabetes Care. 2006;29(9):2114–6. https://doi.org/10.2337/dc06-1136.

3. Cheung N, Mitchell P, Wong TY. Diabetic retinopathy. Lancet. 2010;376:124–36. https://doi.org/10.1016/S0140-6736(09)62124-3.

4. Yau JWY, Rogers SL, Kawasaki R, et al. Global prevalence and major risk factors of diabetic retinopathy. Diabetes Care. 2012;35(3):556–64. https://doi.org/10.2337/dc11-1909.

5. Early Treatment Diabetic Retinopathy Study Research Group. Grading diabetic retinopathy from stereoscopic color fundus photographs—an extension of the modified Airlie House classification: ETDRS report number 10. Ophthalmology. 1991;98(5):786–806. https://doi.org/10.1016/S0161-6420(13)38012-9.

6. Novotny HR, Alvis DL. A method of photographing fluorescence in circulating blood in the human retina. Circulation. 1961;24:82–6. https://doi.org/10.1161/01.CIR.24.1.82.

7. Silva PS, Cavallerano JD, Haddad NMN, et al. Peripheral lesions identified on ultrawide field imaging predict increased risk of diabetic retinopathy progression over 4 years. Ophthalmology. 2015;122(5):949–56. https://doi.org/10.1016/j.ophtha.2015.01.008.

8. Wessel MM, Aaker GD, Parlitsis G, Cho M, D'Amico DJ, Kiss S. Ultra-wide-field angiography improves the detection and classification of diabetic retinopathy. Retina. 2012;32(4):785–91. https://doi.org/10.1097/IAE.0b013e3182278b64.

9. Neubauer AS, Kernt M, Haritoglou C, Priglinger SG, Kampik A, Ulbig MW. Nonmydriatic screening for diabetic retinopathy by ultra-widefield scanning laser ophthalmoscopy (Optomap). Graefe's Arch Clin Exp Ophthalmol. 2008;246(2):229–35. https://doi.org/10.1007/s00417-007-0631-4.

10. Silva PS, Cavallerano JD, Sun JK, Soliman AZ, Aiello LM, Aiello LP. Peripheral lesions identified by mydriatic ultrawide field imaging: distribution and potential impact on diabetic retinopathy severity. Ophthalmology. 2013;120(12):2587–95. https://doi.org/10.1016/j.ophtha.2013.05.004.

11. Schaal KB, Munk MR, Wyssmueller I, Berger LE, Zinkernagel MS, Wolf S. Vascular abnormalities in diabetic retinopathy assessed with swept-source optical coherence tomography angiography widefield imaging. Retina. 2019;39(1):79–87. https://doi.org/10.1097/IAE.0000000000001938.

12. Waheed NK, Rosen RB, Jia Y, et al. Optical coherence tomography angiography in diabetic retinopathy. Prog Retin Eye Res. 2023. https://doi.org/10.1016/j.preteyeres.2023.101206.

13. Domalpally A, Barrett N, Reimers J, Blodi B. Comparison of ultra-widefield imaging and standard imaging in assessment of early treatment diabetic retinopathy severity scale. Ophthalmol Sci. 2021;1(2): 100029. https://doi.org/10.1016/j.xops.2021.100029.

14. Duncan N, Barrett N, Schildroth K, et al. Comparison of standard 7-field, clarus, and optos ultrawidefield imaging systems for diabetic retinopathy (COCO Study). Ophthalmol Sci. 2024;4(3):100427. https://doi.org/10.1016/j.xops.2023.100427.

15. Lee J, Sagong M. Ultra-widefield retina imaging: principles of technology and clinical applications. J Retina. 2016;1(1):1–10. https://doi.org/10.21561/jor.2016.1.1.1.

16. Manivannan A, Plskova J, Farrow A, Mckay S, Sharp PF, Forrester JV. Ultra-wide-field fluorescein angiography of the ocular fundus. Am J Ophthalmol. 2005;140(3):525–7. https://doi.org/10.1016/j.ajo.2005.02.055.

17. Jiang AC, Srivastava SK, Hu M, et al. Quantitative ultra-widefield angiographic features and associations with diabetic macular edema. Ophthalmol Retin. 2020;4(1):49–56. https://doi.org/10.1016/j.oret.2019.08.008.

18. Foote KG, Roorda A, Duncan JL. Multimodal imaging in choroideremia. Adv Exp Med Biol. 2019;1185:139–43. https://doi.org/10.1007/978-3-030-27378-1_23.

19. Akman A, Meditec CZ. In: Akman A, Bayer A, Nouri-Mahdavi K, editors. Optical coherence tomography in glaucoma: a practical guide. 2018. https://doi.org/10.1007/978-3-319-94905-5.

20. Li Y, El Habib Daho M, Conze PH, et al. Hybrid fusion of high-resolution and ultra-widefield OCTA acquisitions for the automatic diagnosis of diabetic retinopathy. Diagnostics. 2023;13(17). https://doi.org/10.3390/diagnostics13172770

21. Lei J, Durbin MK, Shi Y, et al. Repeatability and reproducibility of superficial macular retinal vessel density measurements using optical coherence tomography angiography en face images. JAMA Ophthalmol. 2017;135(10):1092–8. https://doi.org/10.1001/jamaophthalmol.2017.3431.

22. Durbin MK, An L, Shemonski ND, et al. Quantification of retinal microvascular density in optical coherence tomographic angiography images in diabetic retinopathy. JAMA Ophthalmol. 2017;135(4):370–6. https://doi.org/10.1001/jamaophthalmol.2017.0080.

23. Nunes S, Pires I, Rosa A, Duarte L, Bernardes R, Cunha-Vaz J. Microaneurysm turnover is a biomarker for diabetic retinopathy progression to clinically significant macular edema: findings for type 2 diabetics with nonproliferative retinopathy. Ophthalmologica. 2009;223(5):292–7. https://doi.org/10.1159/000213639.

24. Bernardes R, Nunes S, Pereira I, et al. Computer-assisted microaneurysm turnover in the early stages of diabetic retinopathy. Ophthalmologica. 2009;223(5):284–91. https://doi.org/10.1159/000213638.

25. Menean M, Sacconi R, Tombolini B, Fantaguzzi F, Bandello F, Querques G. Combined wide-field imaging in grading diabetic retinopathy. Eye. 2024;38(1):210–4. https://doi.org/10.1038/s41433-023-02666-x.

26. Cogan DG, Kuwabara T. Capillary shunts in the pathogenesis of diabetic retinopathy. Diabetes. 1963;12(4):293–300. https://doi.org/10.2337/diab.12.4.293.

27. Ashton N. Studies of the retinal capillaries in relation to diabetic and other retinopathies. Br J Ophthalmol. 1963;47(9):521–38. https://doi.org/10.1136/bjo.47.9.521.

28. Ong JX, Fawzi AA. Perspectives on diabetic retinopathy from advanced retinal vascular imaging. Eye (Lond). 2022;36(2):319–27. https://doi.org/10.1038/s41433-021-01825-2.

29. Marques IP, Ribeiro ML, Santos T, et al. Patterns of progression of nonproliferative diabetic retinopathy using non-invasive imaging. Transl Vis Sci Technol. 2024;13(5):22. https://doi.org/10.1167/tvst.13.5.22.

30. Ehlers JP, Jiang AC, Boss JD, et al. Quantitative ultra-widefield angiography and diabetic retinopathy severity: an assessment of panretinal leakage index, ischemic index and microaneurysm count. Ophthalmology. 2019;126(11):1527–32. https://doi.org/10.1016/j.ophtha.2019.05.034.

31. Shimouchi A, Ishibazawa A, Ishiko S, et al. A proposed classification of intraretinal microvascular abnormalities in diabetic retinopathy following panretinal photocoagulation. Investig Ophthalmol Vis Sci. 2020. https://doi.org/10.1167/iovs.61.3.34.

32. Ashraf M, Sun JK, Silva PS, Aiello LP. Using ultrawide field-directed optical coherence tomography for differentiating nonproliferative and proliferative diabetic retinopathy. Transl Vis Sci Technol. 2023;12(2):1–7. https://doi.org/10.1167/tvst.12.2.7.

33. Crincoli E, Colantuono D, Zhao Z, et al. Optical coherence tomography angiography for quantitative microvascular assessment in diabetic retinopathy: inter-device and intra-device agreement and correlation with clinical staging. Acta Diabetol. 2022;59(9):1219–27. https://doi.org/10.1007/s00592-022-01921-z.

34. Santos T, Santos AR, Almeida AC, et al. Retinal capillary nonperfusion in preclinical diabetic retinopathy. Ophthalmic Res. 2023;66(1):1327–34. https://doi.org/10.1159/000534553.